w = cumulative weight fraction
z = ratio of oversize product discharge rate to mixed discharge rate, $L > L_p$

Subscripts

E = elutriator flow
F = crystal fines
i = inlet quantities
m = metastable limit
p = crystal product
R = fines loop flow
s = saturation

Greek Letters

β = fines dissolving factor, equal to ratio of mass dissolved to net production
ϵ = crystallizer void fraction
λ = fines dissolving exponential decay factor
ρ = crystal density
τ = mean retention time

Superscripts

$-$ = lower limit of z ramp function
$+$ = upper limit of z ramp function
P = product stream

ACKNOWLEDGMENT

The writers especially wish to acknowledge the efforts of Dr. Erroll Ottens, currently with Stork-Velsen, The Netherlands, who first assembled the classifying crystallizer apparatus and conducted the experimental runs with varying removal port orientation.

The principal investigator is grateful to Dr. Pawel Juzaszek of the Warsaw Technical Institute for his efforts in performing the Mark III CSD simulations. The Polish Educational Ministry is also acknowledged for their support of Dr. Juzaszek.

Appreciation is given to the National Science Foundation, Grants 36517X and ENG 75-04348 and to Kalium Chemicals, Ltd., for financial support of this work.

LITERATURE CITED

Hulburt, H. M., and D. G. Stefango, "Design Models for Continuous Crystallizers with Double Draw-off," *Chem. Eng. Progr. Symposium Ser. No. 95*, **65**, 50 (1969).

Lei, S., R. Shinnar, and S. Katz, "The Stability and Dynamic Behavior of a Continuous Crystallizer with a Fines Trap," *AIChE J.*, **17**, 1459 (1971).

Nuttall, H. E., "Computer Simulation of Steady-State and Dynamic Crystallizers," Ph. D. thesis, Department of Chemical Engineering, Univ. Ariz. (1971).

Randolph, A. D., and M. A. Larson, *Theory of Particulate Processes*, Chapt. 5, Academic Press, New York (1971).

Ibid., Chapt. 8.

Randolph, A. D., G. L. Beér, and J. P. Keener, "Stability of the Class II Classified Product Crystallizer with Fines Removal," *AIChE J.*, **19**, 1140 (1973).

Sherwin, M. B., R. Shinnar, and S. Katz, "Dynamic Behavior of the Well-Mixed Isothermal Crystallizer," *ibid.*, **13**, 1141 (1967).

Song, Y., and J. M. Douglas, "Self-Generated Oscillation in Continuous Crystallizers: Part II," *ibid.*, **21**, 924 (1976).

Manuscript received December 6, 1976; revision received April 22, and accepted April 27, 1977.

Crystal Size Distribution Dynamics in a Classified Crystallizer:

Part II. Simulated Control of Crystal Size Distribution

JAMES R. BECKMAN

and

ALAN D. RANDOLPH

Department of Chemical Engineering
University of Arizona
Tucson, Arizona 85721

Control of sustained limit-cycle instability in crystal size distribution (CSD) was simulated for a class II (high yield) crystallizer equipped with a fines destruction system and product classifier. Control was simulated by proportional control of nuclei density using fines destruction rate as the manipulated variable. The control constant necessary to eliminate instability was theoretically predicted and agreed with the constant found via simulation. Poorer control of CSD (inability to completely eliminate limit cycles) was predicted using slurry density and slurry withdrawal rate as the measured and manipulated variables, respectively. Development of techniques for fine crystal population measurements to estimate nuclei density are necessary for implementation of the former control scheme. The suggested nuclei density control scheme is effective both in minimizing CSD transients and for elimination of instability.

SCOPE

Some industrial class II crystallizers operating with fines destruction, clear liquor advance and product classification (the complex crystallizer) experience sustained limit-cycle behavior in crystal size distribution. As described in Part I of this series, both an industrial and a laboratory crystallizer producing potassium chloride were observed to develop cycling CSD's under certain operating conditions. Such unstable CSD behavior was not a result of outside disturbances but was caused by an interaction between nucleation rate and process configuration.

Control of sustained limit-cycle behavior in CSD is of industrial importance. Instability affects production by

Correspondence should be directed to Dr. Randolph. James R. Beckman is at the California State University, Northridge, California.

loss in product, overloading of dewatering equipment, exacerbated equipment fouling, and off-specification product.

Previous investigators have not tackled the control problems associated with realistically modeled industrial crystallizers. Idealized assumptions such as point fines trap, mixed product removal, class I yield behavior, high kinetic order (necessary for instability), and unmeasurable control variables have limited the application of previous CSD control studies. There remains a need for identification of control philosophies which can reduce or eliminate sustained limit-cycle behavior of CSD in industrial crystallizers of complex configuration. It was the purpose of this study to develop control philosophies both from theoretical grounds and from computer simulation which will aid in the design and control of industrial complex crystallizers.

CONCLUSIONS AND SIGNIFICANCE

Computer simulator CYCLER was developed to simulate the dynamics and control of class I and II crystallizers equipped with fines destruction, clear liquor advance, and product classification. The simulator was used extensively throughout this study in the analysis of experimental work and the development of control philosophies. The most efficient control philosophy found for complex class II crystallizers was proportional control of nuclei density by manipulation of the fines destruction flow rate. Nuclei density was estimated by a pseudo steady state linear extrapolation of the log of calculated particle densities at various small but finite particle sizes. Such particle population data might be obtained experimentally using electronic instruments, for example, zone sensing or laser light scattering types. Even during highly unstable conditions, the calculated population densities obeyed an exponential pseudo steady state distribution. This extremely important conclusion was observed experimentally in Part I and enhances the possibility for practical application of the fines destruction control scheme.

The simulated control constant needed to stabilize an inherently unstable complex crystallizer was identical to the value estimated from the earlier linearized spectral analysis study of Randolph et al. (1973), thus confirming the validity of the quasi steady state assumption for the fines distribution. Simulation of an industrially used control scheme involving manipulation of product removal rate based on measurement of slurry density showed that such a control strategy was sensitive to measurement errors, would not eliminate excessive cycling, and was worse than no control at all for compensation of nucleation disturbances.

Several researchers have investigated the CSD dynamics of crystallizers, specifically, sustained limit-cycle behavior of CSD. The crystallizer models investigated ranged from simple mixed suspension mixed product removal (MSMPR) to more complex units having fines destruction, clear liquor advance, and product classification (the complex crystallizer). Crystallization systems considered varied from slow growth rate kinetics (class I, where residual supersaturation is appreciable) to fast growth systems (class II, where growth rate is constrained only by rate of make per unit crystal area). The reader is referred to Part I of this study for specific details of the theoretical aspects of crystallizer process dynamics.

Previous dynamic studies have clearly set the stage for continued research in the area of control. Control studies are divided into two categories since there are two dynamic modes that a crystallizer may experience, namely, dynamics due to external disturbances or sustained limit-cycle behavior which is self-perpetuated.

Few researchers have investigated control of crystallizers. Han (1967) analyzed the stability of class I MSMPR crystallizers. He investigated a feed forward scheme which controlled supersaturation using feed rate as the manipulated variable. Good control was predicted when the crystallizer was operated in a stable region. However, the controller did not reduce sustained limit-cycle behavior in unstable regions. Timm and Gupta (1970) analyzed stability control of class II MSMPR crystallizers. They investigated control of variables such as the zeroth and second moments of the population distribution using fines seeding and destruction as the manipulated variable. (The zeroth moment is a measure of the total number of particles within the crystallizer, while the second moment is a measure of the total crystal surface area.) They found that by controlling the zeroth moment, sustained limit cycling could be eliminated. On the other hand, control of the second moment might drive a normally stable crystallizer unstable. Unfortunately, the measurement of total number or total area of particles within a dynamic industrial crystallizer is a difficult if not impossible task using current on-line particle measurement technology. Lei, Shinnar, and Katz (1971) studied the control of a class I MSMPR crystallizer equipped with a point fines trap. They investigated control of fines crystal area by manipulating either throughput rate or fines destruction. It was found that an unstable system could be stabilized by manipulation of throughput rate but not by manipulation of fines destruction rate.

Significantly, all previous control studies used the MSMPR configuration as the crystallizer model. Such a model requires an unreasonable nucleation/growth rate kinetics sensitivity (not observed in experimental nucleation studies) for the system to become unstable. Part I of this study convincingly demonstrates that size dependent residence time, not nucleation sensitivity, is the prime cause of CSD instability as observed in industrial crystallizers of complex configuration. Specifically, the interaction of product classification with accelerated fines removal (fines dissolving or clarified liquor overflow) results in such instability in otherwise stable regions of nucleation/growth rate sensitivity.

The present study addresses itself to the CSD stabilization and control of realistic complex crystallizers as actually exist in industrial practice.

SYSTEM EQUATIONS

The important balances which must be considered to describe crystallization dynamics include solute, solid phase, and crystal population. The following theoretical

development was performed on a class I complex crystallizer which included fines destruction, product classification, and clear liquor advance. A schematic of the process flow is illustrated in Figure 1. A class I system was selected, since it represents the most general crystallization system. Class II systems are merely a limiting case of class I behavior as yield increases.

POPULATION BALANCE

Consider the following population density balance on solid particles:

$$V_L[B(L) - D(L)] = \frac{\partial(nV)}{\partial t} + \frac{\partial(GnV)}{\partial L} + h(L)n\,Q_p \tag{1}$$

Equation (1) shows that net particles generated at any size must either accumulate in the crystallizer, grow into or out of size ranges, or be removed from the system by fines destruction, clear liquor advance, or product removal. The term $h(L)$ is the withdrawal function in size which describes all possible avenues of particle removal. A convenient parameterization of $h(L)$ which captures the flavor of a complex crystallizer, yet results in tractable mathematics, is as follows:

$$h(L) = \begin{cases} R & 0 \leq L \leq L_F \\ a & L_F \leq L \leq L_p^- \\ a + \dfrac{z-a}{(L_p^+ - L_p^-)} \cdot (L - L_p^-) & L_p^- \leq L \leq L_p^+ \\ z & L_p^+ \leq L \end{cases} \tag{2}$$

Equation (1) is simplified by making a few assumptions and definitions. Let V represent slurry volume, not clear liquor. Since the crystallizer operates with level control, slurry volume will be constant during transients in slurry density. Define the liquor void fraction in the crystallizer to be the ratio of liquor to slurry volume. Thus

$$\epsilon_c = V_L/V \tag{3}$$

Define residence time to be the ratio of slurry volume to volumetric flow rate of the product stream. Assume growth rate G is independent of crystal size. Further, the left-hand side of Equation (1) represents the net nuclei birth generation as a function of size. This distributed birth function is extremely difficult to work with and, in most cases, completely unknown. Therefore, the conventional lumped birth model of nuclei having zero size is assumed. The resulting birth flux B^0, which is the semi-infinite integral of the net birth function, is eliminated from Equation (1) only to become a part of the boundary condition. Equation (1) can thus be simplified to

$$0 = \frac{\partial n}{\partial t} + G\frac{\partial n}{\partial L} + \frac{h(L)n}{\tau} \tag{4}$$

The boundary condition in size for Equation (4) is obtained via a nuclei kinetics assumption. The slurry dependent power law model as described by Randolph and Larson (1971) is used to represent the birth flux at zero particle size:

$$B^0 = k_N\, G^i\, M_T^j \tag{5}$$

The particle flux at nuclei size is thus

$$B^0 = n^0 G \tag{6}$$

A combination of Equations (5) and (6) yields the boundary condition for the population density balance [Equation (4)]:

$$n^0 = k_N \epsilon_c\, G^{i-1}\, M_T^j \tag{7}$$

SOLUTE BALANCE

The solute balance equation is derived by setting all salt inputs in both dissolved and solid form equal to all salt outputs and accumulation. Figure 1 is a schematic representation used for the solute balance. After some simplification coupled with a solids-phase balance, the solute balance becomes

$$\frac{F}{\tau}(C_F - \gamma C) + \frac{P_R}{V}\left(1 - \frac{C}{\rho}\right)\left(\frac{R - \gamma F}{R-1}\right) = (\rho - C)\cdot k_A G\, m_2/2 + \epsilon_c \frac{dC}{dt} \tag{8}$$

GROWTH RATE

Growth rate was assumed to be proportional to supersaturation:

$$G = k_g(C - C_s) \tag{9}$$

Equations (4), (7), (8), and (9) form a closed set of relationships needed for the dynamic simulation.

SOLUTION METHODOLOGY OF CYCLER

Previous investigators have suggested ways for solving the population-balance equation. Nuttal (1971) solved the balance equations by discretizing the population balance PDE and solving via Heun's method (improved Euler). Nyvlt and Mullin (1970) solved the crystallization equations using particle age as the independent variable coupled with Monte-Carlo product removal. Shields (1976) integrated the population density balance in differential size to generate a matrix of particle densities at specific sizes. He then solved the system of ODE's using Euler's method.

A novel approach to solving the population balance equation was developed in the present study. It was assumed that during small time increments, the growth rate and nuclei boundary condition could be considered constant at some average value. Although both were functions of time, they in fact changed little during a small time increment (which was still much longer than the in-

SCHEMATIC OF COMPLEX CRYSTALLIZER WITH FINES DESTRUCTION, CLEAR LIQUOR ADVANCE AND PRODUCT CLASSIFICATION

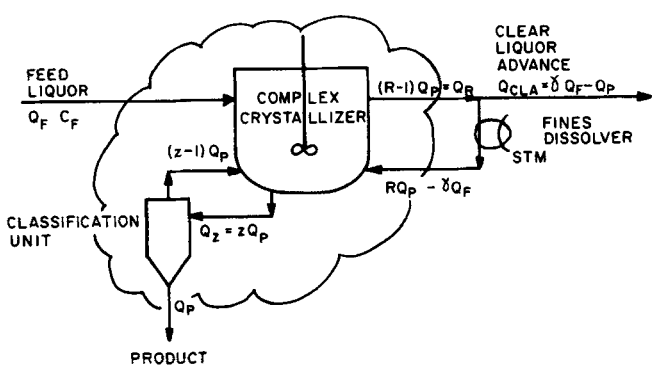

Fig. 1. Schematic of complex crystallizer.

cremental time step required for numerical stability with a finite difference solution). Most simulations showed little difference in transient behavior when the time step was increased from 10 to 20 min. To better approximate the solution, average values of growth rate, nuclei density, and slurry density were used over any one time step. Convergence of these values was required before the next time step was considered. The time variant population balance was solved by sequentially starting and stopping the solution after each time step. The final solution, after a time step was completed, became the initial condition for the next time step calculation.

For small time increments with constant coefficients, Equations (4) and (7) become

$$\frac{\partial n}{\partial t} + \overline{G}\frac{\partial n}{\partial L} + \frac{h(L)n}{\tau} = 0 \tag{10}$$

$$\overline{n^0} = \overline{\epsilon_c} k_N \overline{G}^{i-1} \overline{M_T}^j \tag{11}$$

Equation (10) is converted to a more tractable form by dividing each term by the population density function n with $y = \log n$. Equations (10) and (11) become

$$\frac{\partial y}{\partial \theta} + \overline{G}\,\tau\frac{\partial y}{\partial L} + h(L) = 0 \tag{12}$$

$$\overline{y^0} = \log k_N \overline{\epsilon_c} + (i-1)\log \overline{G} + j \log \overline{M_T} \tag{13}$$

where $\theta = t/\tau$ is a dimensionless time. Equation (12) with Equation (13) has an analytical solution which was found by using Laplace transforms twice, first in size, then in time. Thus

$$\begin{aligned} y(L,t) = {} & \overline{y}^0 - \frac{RL}{\overline{G}C} \\ & + \left[y^{IC}(L - \overline{G}t) - \overline{y}^0 + \frac{R}{\overline{G}\tau}(L - \overline{G}t) \right] u_{\overline{G}t}(L) \\ & + \left[\frac{R-a}{\overline{G}\tau}(L - L_R) \right] u_{L_R}(L) \\ & + \left[\frac{-R+a}{\overline{G}\tau}(L - L_R - \overline{G}t) \right] u_{L_R+Gt}(L) \\ & - [\alpha(L - L_p^-)^2]\, u_{L_p^-}(L) \\ & + [\alpha(L - L_p^- - \overline{G}t)^2]\, u_{L_p^-+\overline{G}t}(L) \\ & + [\alpha(L - L_p^+)^2]\, u_{L_p^+}(L) \\ & - [\alpha(L - L_p^+ - \overline{G}t)^2]\, u_{L_p^++\overline{G}t}(L) \end{aligned} \tag{14}$$

where

$$\alpha = \frac{z-a}{2\overline{G}\tau\,(L_p^+ - L_p^-)}$$

The initial condition at each time step y^{IC} became too cumbersome to handle analytically. Therefore, y was solved at specific points in size. These points had their own initial conditions from the previous time step so that a new updated value of y could be calculated at the same points.

After the population balance is solved, during any time step, the solute balance is solved in order to update estimates of growth rate G and solute concentration C. After discretizing the solute balance [Equation (8)] coupled with the growth rate expression [Equation (9)], we can solve the solute concentration. These equations were decomposed and solved in the following sequence:

$$C = G_5 - \sqrt{G_5^2 - G_6} \tag{15}$$

$$G_1 = FC_F + \rho k_v m_{3R}\left(\frac{R - \gamma F}{R-1}\right) + \frac{\epsilon_c C_o}{\theta} \tag{16}$$

$$G_2 = F\gamma + k_v m_{3R}\left(\frac{R-\gamma F}{R-1}\right) + \epsilon_c/\theta \tag{17}$$

$$G_3 = \tau\rho\, k_A\, m_2/2 \tag{18}$$

$$G_4 = G_3/\rho \tag{19}$$

$$G_5 = \left[\frac{G_2}{k_g} + G_3 + G_4 C_s\right] \Big/ 2G_4 \tag{20}$$

$$G_6 = \left[\frac{G_1}{k_g} + G_3 C_s\right] \Big/ G_4 \tag{21}$$

After we solve for solute concentration, growth rate can be calculated as

$$G = \frac{G_1 - G_2 C}{G_3 - G_4 C} \tag{22}$$

In this manner, both class I and II systems can be handled by the simulator.

CONTROL

Randolph et al. (1973) published a definitive paper which outlined the stability characteristics for a class II complex crystallizer. Figure 2 in Part I of this study [after Randolph et al. (1973)] shows the stability boundary for an idealized complex crystallizer. In the figure, stability is assured when the operating point of a complex crystallizer lies to the left of the oblique stability boundary line which is determined by the process operating conditions. Processes that lie to the right of their characteristic stability line will exhibit sustained limit-cycle behavior in CSD. A process lying to the right of its stability boundary can only become stable if its effective fines destruction rate is reduced to the stable operating value R_s.

It was theoretically determined in this present study that sustained limit-cycle behavior can be eliminated without moving the actual process operating point by proportional control of nuclei density n^0 using fines destruction rate as the manipulated variable. The proportional controller constant K_c which guarantees control is calculated by theoretically moving the process operating point back to the stability line. Thus

$$K_C \geq \left(1 - \frac{R_s}{\overline{R}}\right) \Big/ (i-1) \tag{23}$$

Details involved in the derivation of minimum K_C are given in the Appendix. In this case, steady state control action is assumed; that is, no dynamic lags in the control or fines removal systems are considered. The validity of the latter assumption was borne out by both CYCLER calculations and experimental nuclei measurements (see Part I).

RESULTS

The control study used the laboratory crystallizer as described in Part I as the base case This was done for two reasons. First, the laboratory crystallizer did cycle, so it represented a physically realizable unstable complex crystallizer. Second, the control study will act as the groundwork for a future real-time experimental control study of the laboratory crystallizer. The specific kinetics constants k_N, i, and j [as per Equation (5)] from the experimental laboratory crystallizer of Part I were used for the examples of the present control study.

Since Part I proved the existence of sustained limit-cycle behavior in CSD, Part II therefore deals with the reduction

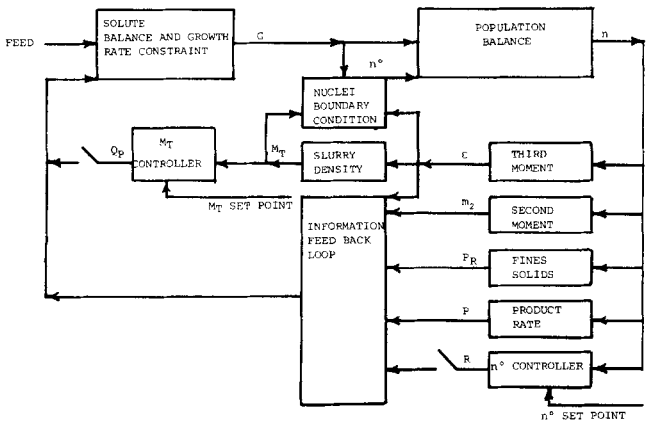

Fig 2a. Information flow diagram determining CSD.

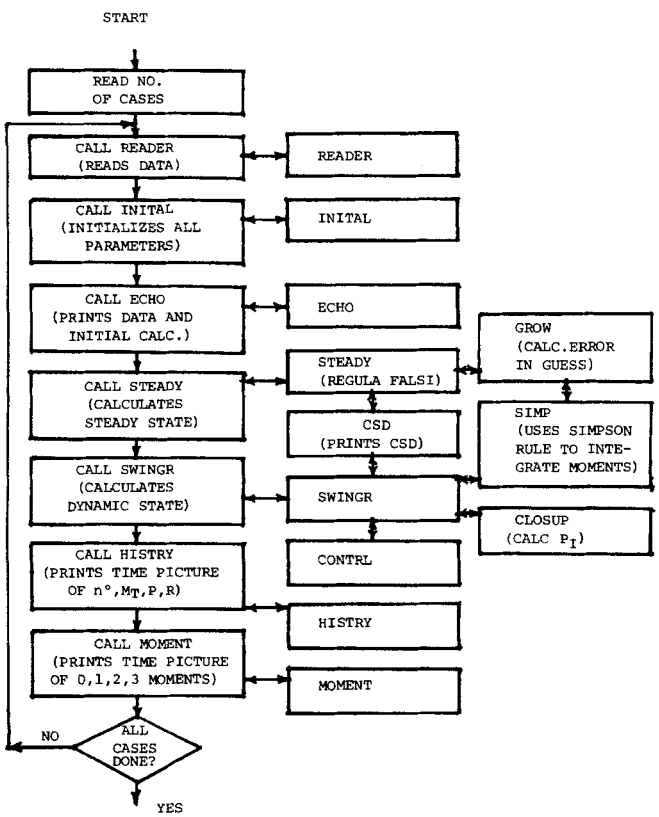

Fig. 2b. Information flow diagram for program CYCLER.

and elimination of this cycling phenomena. Computer program CYCLER was used to accomplish this task. CYCLER not only simulates the dynamic behavior of complex crystallizers but also simulates their controlled behavior. CYCLER is equipped with a controller subroutine which, when called by the dynamic section of the program, adjusts the values of the manipulated process variable based on the error of the desired controlled variable. The action is not continuous but is piecewise continuous in time. The dynamic section of CYCLER solves the population balance equation over small time intervals. It is at the end of each of these steps that control action is called upon to change the value of the manipulated process variable. In the present study, cycle periods of from 300 to 400 min were typically experienced in the control simulation of the laboratory crystallizer. A computer time step of 10 min was used for computer economy which resulted in about 35 resets/cycle. Halving the time step did not significantly alter the results. Therefore, CYCLER does numerically simulate a

Table 1. Identification of Subfunctions Used in Program Cycler

Subfunction	Purpose
Closup	Calculates and prints P_I over one cycle
Contrl	Changes value of manipulated variable based on control variable error
CSD	Prints fines trap, crystallizer, and product CSD's and cumulative weight fractions
Echo	Prints all read in data and initialized parameters
Grow	Calculates error in steady state growth rate assumption
Histry	Prints time picture of n^o, M_T, P, and R
Inital	Initializes all parameters used in CYCLER
Moment	Prints time picture of zeroth, first, second, and third moments and solute concentration
Reader	Reads in all data
Simp	Uses Simpson's rule to integrate moments
Steady	Calculates steady state CSD by guessing growth rate via Regula Falsi method
Swingr	Calculates dynamic CSD using Equations (14) to (22)

continuous controller. An overall information flow diagram for CYCLER showing both process dynamics and control functions is shown in Figures 2*a* and 2*b*. The numerical functions of the subroutines shown in Figure 2*b* are identified in Table 1.

VERIFICATION OF CYCLER

Since the computer simulator CYCLER was the main tool used in this control study, it was imperative to insure that CYCLER predicted stable and unstable behavior in accordance with the previous analytical stability study [Randolph et al. (1973)]. Figure 2 in Part I was chosen as the test basis because the parametric values used in its construction were close to those found experimentally in the laboratory crystallizer. The physical realizability of the laboratory crystallizer coupled with the theoretical soundness of the previous linearized spectral density analysis made this a logical choice for testing the validity of simulator CYCLER.

Figure 3 of this study compares the stability boundary line of Randolph et al. (1973) with CYCLER produced frequency and performance index. Figure 3 shows that the farther the computed operating point moves to the right of the stability boundary, the larger becomes the performance index and the frequency, therefore verifying the stability prediction of CYCLER.

A performance index P_I was needed to quantify the deviation from steady state of the cycling system. The index as defined in this study is the root-mean-square relative error of the cumulative weight fraction at 200 μm size in the product stream:

$$P_I \equiv \left[\int_0^1 \left\{ \frac{W(200\ \mu\text{m})}{W(200\ \mu\text{m})} - 1 \right\}^2 d(wt) \right]^{1/2} \quad (24)$$

P_I is a positive quantity which drives to zero as cycling is reduced.

NUCLEI CONTROL STUDY

Figure 4 shows the performance index as a function of controller gain as simulated by CYCLER. P_I decreases with increasing K_c to become nil at about 0.25. This compares exactly with the K_c predicted from Equation (23).

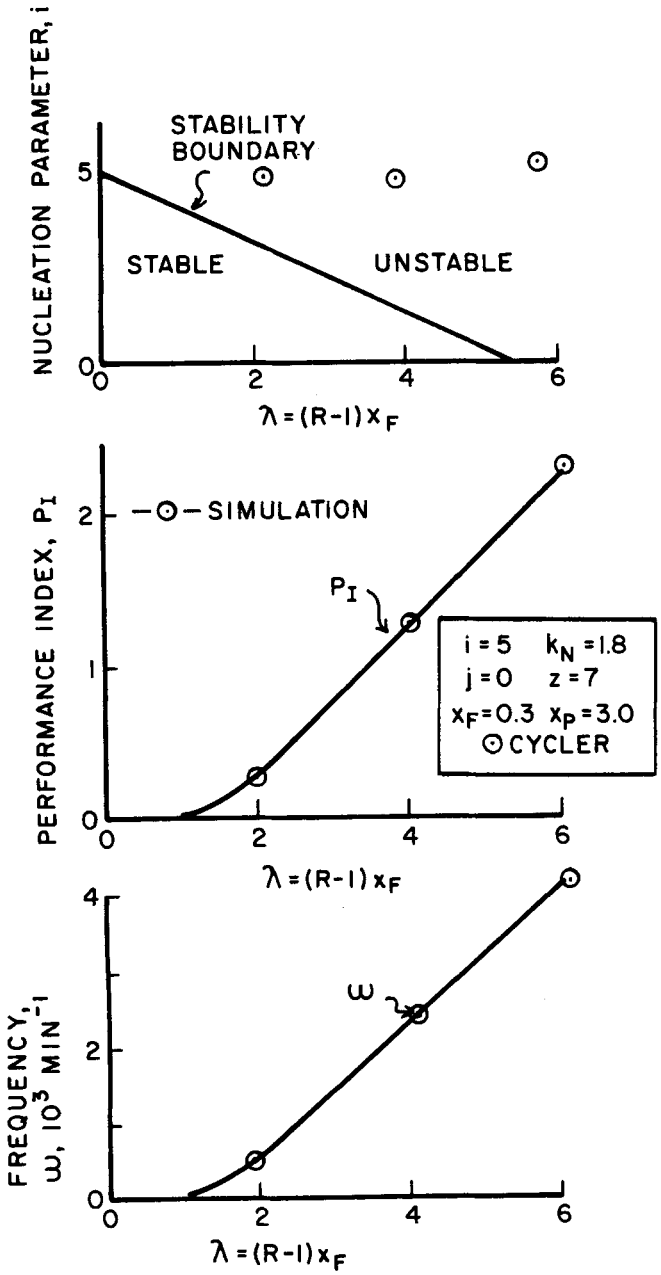

Fig. 3. Comparison of linearized and CYCLER produced stability predictions.

Thus, CSD instability is completely eliminated by this control action.

Figure 5 shows two curves which were generated by CYCLER. One was developed assuming the exact (computed) value of nuclei density as the controlled variable. The other was developed assuming imperfect knowledge of the nuclei density. CYCLER used a random number generator to simulate 50% relative white-noise error in the measurement of nuclei density. Even at 50% random error in simulated nuclei density, this control scheme demonstrated excellent controllability in reducing the percent performance index from 300% to nil.

Figure 5 also shows that the P_I can be reduced to nil for K_c greater than 0.3 for the case of perfect knowledge of nuclei density. When 50% random error was introduced in nuclei density, the P_I at first reduced to nil at $K_c = 0.3$ and then increased slowly to larger values as K_c increased owing to amplification of the random error. In any case, CSD cycling was effectively eliminated.

To further demonstrate the usability of this control scheme, a more practical approach was taken wherein

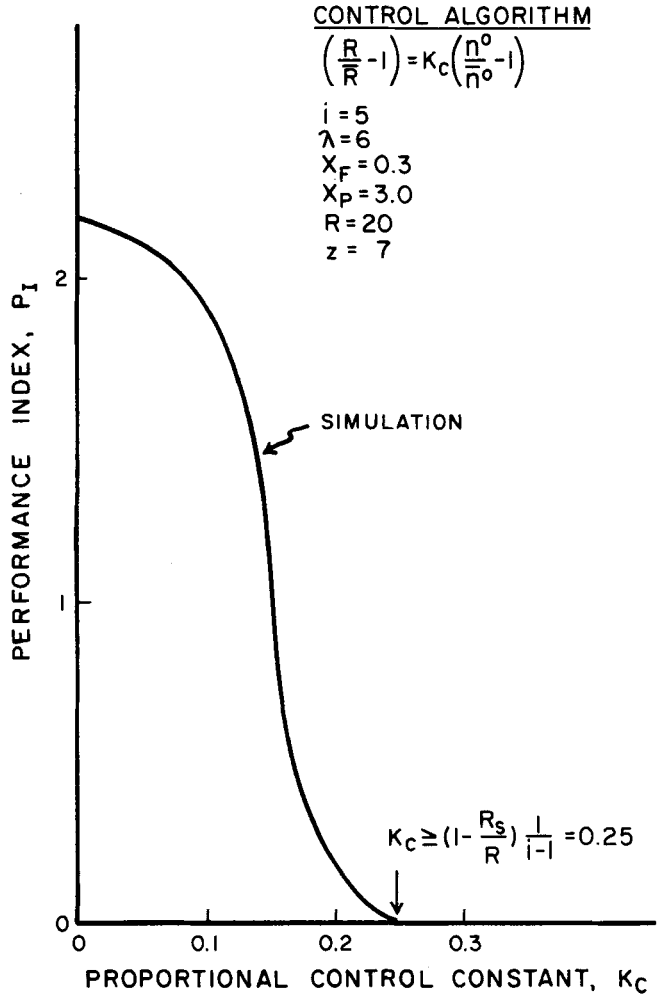

Fig. 4. Stabilization of CSD using proportional control of nuclei density.

nuclei density was estimated by extrapolation of small particle size data to zero size. It must be remembered that n^0 refers to the nuclei density at zero particle size. No instrument analyzes zero size particles. However, electronic particle counters such as used in the laboratory investigation of Part I do analyze particle densities at very small particle sizes (for example, 10 to 100 μm). Under steady state conditions, a plot of log of particle density vs. particle size for particles up to L_F is linear having the log of nuclei density as the intercept at zero size. Using linear least-squares extrapolation, we can estimate nuclei density by Equation (25):

$$n^0 = \exp\left[\frac{\Sigma y \, \Sigma L^2 - \Sigma L \, \Sigma yL}{p \, \Sigma L - (\Sigma L)^2}\right] \qquad (25)$$

Figure 6 shows the P_I reduction with increases in K_c when n^0 was estimated by a least-squares extrapolation using population densities at sizes 20, 25, 30, and 40 μm positions. This selection was made since it approximates the cube root of two particle size sequence which an electronic particle counter would actually measure.

The response line in Figure 6 generated by assuming a pseudo steady state for small particles is identical to the response line of Figure 5 where nuclei density was precisely known. These curves are identical even in the range of high oscillatory behavior (for example, $0 \leq K_c < 0.3$).

These calculations indicate that the fines distribution in a complex crystallizer maintains a quasi steady state exponential distribution even when the entire distribution of larger sizes is in a cycling mode. This observation was confirmed in the experimental study (Part I), where

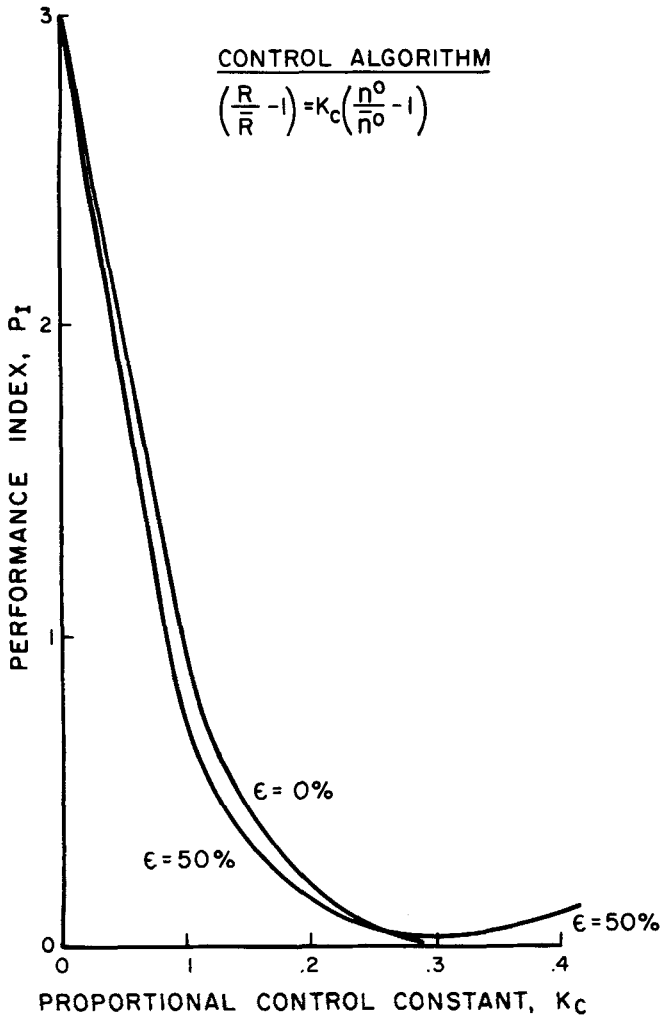

Fig. 5. Control of an unstable CSD by controlling nuclei density with fines destruction rate.

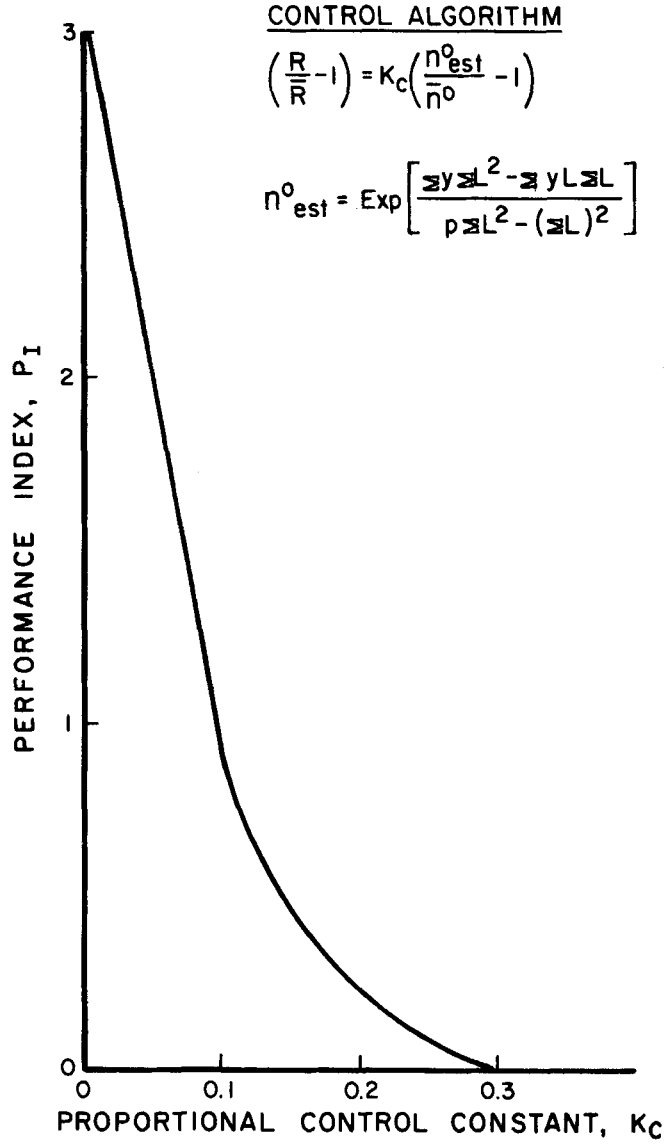

Fig. 6. Control of unstable CSD by extrapolation of fine crystal populations.

straight-line, semilog fines distributions were always measured even with extremely unstable CSD's. This fortuitous circumstance is, of course, due to the about twentyfold decrease in mean retention probability ($R \geq 20$) of the fines vis-a-vis product crystals. Therefore, the pseudo steady state assumption appears to be a valid practical technique in estimating nuclei density even during transient operation. This observation could make this control scheme a practical reality in stabilizing inherently unstable industrial complex crystallizers.

To further test the effectiveness of CSD control by manipulation of fines destruction rate, other set point control sizes were simulated by CYCLER. Selected population densities at 30, 60, and 200 μm were investigated using fines destruction rate as the manipulated variable. The results are plotted on Figure 7 along with the cycle frequency of all the runs. From Figure 7 it is clear that control improves with the desired control set point at lower particle size. Also at lower set point size, the K_c required to reduce P_I to nil is less. Reduction in values of K_c should minimize the capital and operating costs of the control equipment needed to adjust the fines destruction pumping rate. The relationship between controller gain and the fines set point size is intuitively correct; as the set point size is reduced, the removal system is more effective in catching up with any nuclei disturbances. Figure 7 also shows the frequency of the various control schemes as a function of K_c. For the cases where the control set point size is within the fines destruction zone ($L_F = 60$ μm), the frequency tends to increase to a maxima at about $K_c =$ 0.15, then decrease with increasing K_c to perhaps zero. The frequency curves are not complete owing to the unreliability in estimating the cycle period as amplitudes of all process responses became undetectably small. On the other hand, control at 200 μm generated increases in frequency with increases in K_c. This result was probably due to the overshoot caused by high values of K_c coupled with the dead time associated with a control point lying outside the fines destruction zone. Note that when the nuclei density control set point lies outside of the effective fines destruction size range [for example, control at n (200 μm) with $L_F = 60$ μm], cycling cannot be completely eliminated even with the optimum control setting. This result is compounded with measurement error in the population density set point.

STABILIZATION OF CSD BY CONTROL OF SLURRY DENSITY

Owing to difficulties in analysis and application of a workable control algorithm, industrial complex crystallizers have traditionally been operated in the inherently stable region as depicted in Figure 2 of Part I. Often this is done at the price of producing a wider distribution with more fines. Of course, in any control scheme quantities which are either controlled or manipulated must be easily

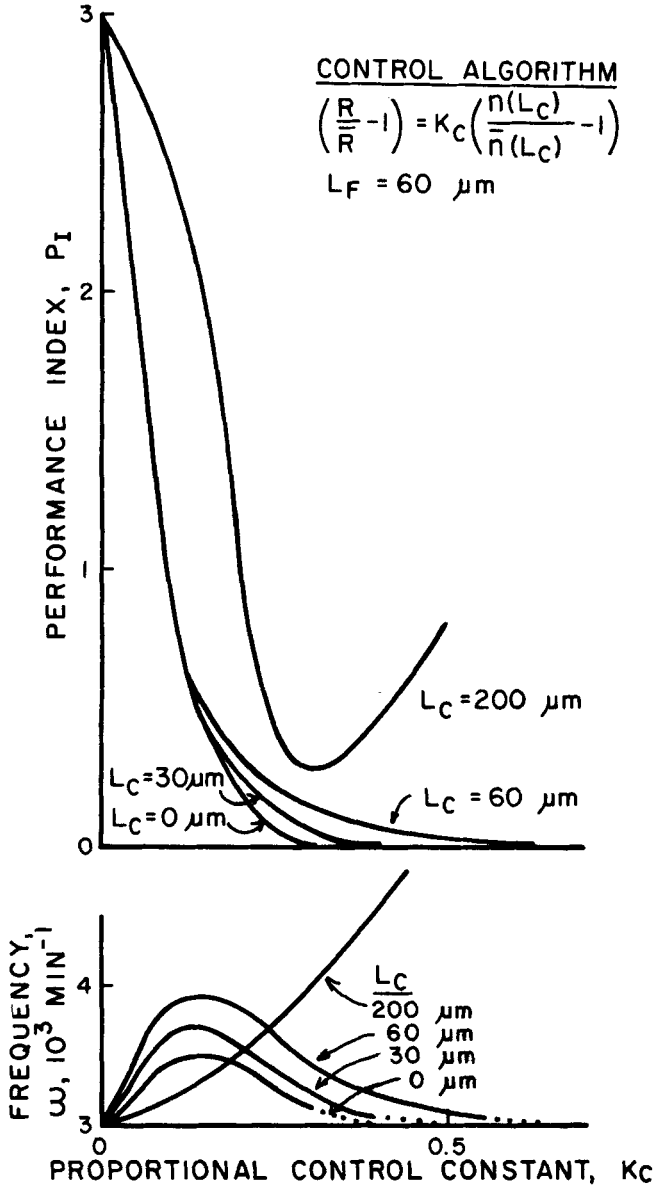

Fig. 7. Control of unstable CSD using population density set points at finite sizes.

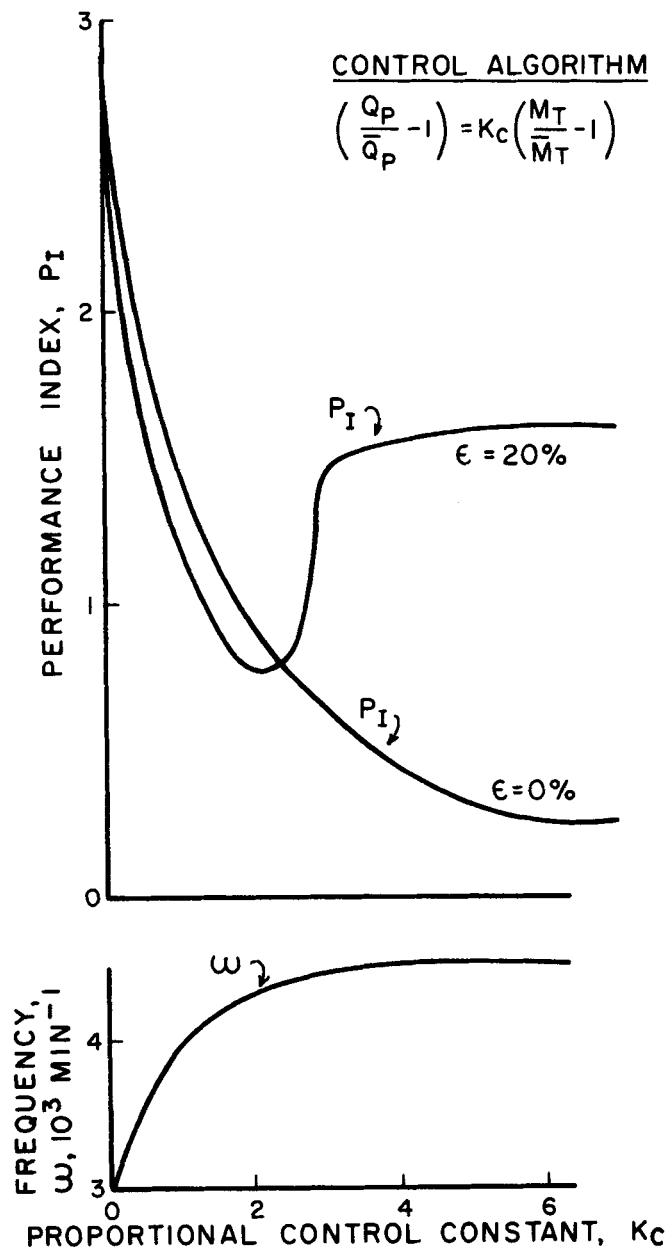

Fig. 8. Control of unstable CSD by stabilization of slurry density.

and readily observed. This difficulty of observability is one of the major faults of control schemes which have been theoretically investigated. It is common industrial practice to measure total solids concentration (for example, with differential pressure measurements) and attempt to stabilize slurry density M_T. It has been posed that such control of slurry density within the crystallizer by using product pumping rate Q_P as the manipulated variable will eliminate sustained limit-cycle behavior in CSD (Shields, 1976). However, little success has been achieved in regard to stabilizing the CSD.

Figure 8 shows a simulation of an unstable crystallizer with CSD control attempted by controlling M_T with manipulation of Q_P. *If* we assume perfect knowledge of M_T, the performance index P_I could be reduced to about 20% for this unstable case, but cycling could not be eliminated. In general, industrial crystallizers have difficulty in measuring the slurry density to within 20% absolute accuracy. Using an estimate of M_T with a 20% random error, Figure 8 shows that as the controller constant is increased to about 2.0, P_I drops from 300 to 80% then rapidly rises to a value of 160% as K_c increases. The leveling off of the P_I at higher gains was only due to the fact that changes in the removal rate Q_P were bounded in the simulation at

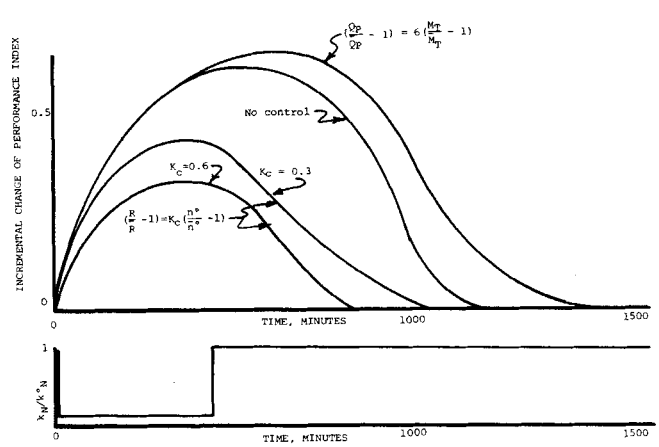

Fig. 9. Effectiveness of CSD control schemes in reducing transient upsets.

± 20% of the steady state removal pumping rate. In some industrial situations, attempts at stabilization of M_T, while effective in leveling out load changes in dewatering equipment, are virtually fruitless in stabilizing CSD.

CONTROL OF CSD TRANSIENTS

The emphasis of this control study has been the identification of control strategies to minimize or eliminate CSD cycles in an inherently unstable system. The question can be asked: "Are control schemes which might stabilize CSD effective in reducing the CSD disturbances caused by externally induced upsets?" This study does not definitively answer this question; however, the proposed nuclei density control scheme was compared with the slurry density stabilization scheme for a simple pulse disturbance in nucleation rate. The case studied represented a stable crystallizer with the nucleation rate constant k_N severely reduced for a period of approximately two retention times. Parameters for the laboratory crystallizer were used, except the amount of classification was reduced to give a stable CSD. (Such a case might simulate the disturbance caused by inadvertent addition of dilution water.) Figure 9 shows the instantaneous contribution of the performance index for these two cases (observed at any given time) compared with the case of no control. The nuclei density control scheme, using the minimum gain for CSD stabilization, results in significantly less deviation of CSD as measured by the chosen performance index. This deviation is further reduced by increasing the gain beyond the minimum stabilization value. Note that the slurry density scheme is worse than no control at all. This is to be expected, as the solids density is not significantly perturbed until after the nuclei disturbance has disappeared; corrective action is then too late and further disturbs the system.

CONCLUDING REMARKS

Of the two CSD control schemes simulated in this study, namely nuclei density and slurry density control, the former is much superior for the stabilization of cycling CSD's while still being effective in reducing disturbances caused by nucleation upsets. Slurry density stabilization is totally ineffective in reducing the effects of nucleation disturbances and quite likely would exacerbate such CSD upsets. However, slurry density control can be implemented with current crystallizer controls. The implementation of nuclei density control would require development of sophisticated on-line particle size measurements typically in the 10 to 100 μ size range. Fortuitously, the ideal location for such fine crystal particle size measurement would be in the fines removal circulation stream from which large size product crystals had been excluded. Electronic instruments of the zone sensing type might be used (as in this experimental study, Part I), but serious problems of orifice plugging, fouling, coincidence, and lack of conductivity might be encountered in some systems. Electronic particle analyzers based on the principle of low angle scattering of a laser light beam might operate in an industrial environment with less problems due to the above factors. Such instruments have recently been put in use for the control of grinding circuits (Bay et al., 1975). In any case, crystal measurements in the necessary size range would be virtually precluded in dirty systems containing finely suspended emulsions, gangue, or froth. The potassium chloride-brine system studied in Part I while admittedly a laboratory system, would not be subjected to any of the above limitations.

In summary, control of nuclei density using estimates of the population density, obtained by extrapolation of fine crystal populations together with manipulation of fines removal rate, appears to be a potentially attractive technique for control and stabilization of CSD in industrial crystallizers of complex configuration. The problem of CSD instability could be attacked in two ways as suggested in Parts I and II of this study, namely, modify the process configuration or implement a stabilizing control scheme. The former approach might result in a less attractive product (a wider distribution with more fines), while the latter would incur significant development costs but would preserve the desirable narrow CSD. The choice between these two approaches (or continue with cyclic operation) would have to be decided for each case based on economic considerations.

ACKNOWLEDGMENT

Appreciation is given to the National Science Foundation, Grant ENG 75-04348, for financial support of this work.

NOTATION

a = sedimentation factor
B^0 = birth rate at zero size number/(cm^3)(min)
$B(L)$ = birth distribution function, number/(cm^3)(μm)(min)
C = solute concentration, g/cm^3
C_F = feed liquor solute concentration, g/cm^3
C_o = solute concentration initial condition, g/cm^3
C_s = saturated solute concentration, g/cm^3
$D(L)$ = death distribution function, number/(cm^3)(μm)(min)
F = ratio of feed rate to produce rate, Q_F/Q_P
G = diameter growth rate, μm/min
$H(\xi)$ = deviation withdrawal $h(\xi) - \overline{h}(\xi)$
$\overline{H}(\xi)$ = effective withdrawal
$h(\xi)$ = withdrawal function
i = kinetic power of growth rate in nucleation birth function
j = kinetic power of solids concentration in nucleation birth function
k_A = area shape factor
K_c = proportional control constant
k_g = growth rate kinetic constant (μm)(cm^3)/(g)(min)
k_N = nucleation rate kinetic constant
k_V = volumetric shape factor
L = particle size, μm
L_F = upper limit of fines destruction, μm
L_p^- = product ramp lower limit, μm
L_p^+ = product ramp upper limit, μm
m_2 = second moment in crystallizer
m_{3R} = third moment in fines trap
M_T = slurry density in crystallizer, g/l
n^0 = nucleation density at zero size, number/(cm^3)(μm)
n = population density function, number/(cm^3)(μm)
N = population deviation, $n/n - 1$
P = solids product rate, g/min
p = number of sample points
P_I = performance index
P_R = solids rate destroyed in fines destruction system
Q_{CLA} = slurry flow rate of clear liquor advance, cm^3/min
Q_F = slurry based liquor feed rate, cm^3/min
Q_P = slurry based liquor product rate, cm^3/min
Q_R = slurry based fines destruction rate, cm^3/min
Q_z = slurry based classifier feed rate, cm^3/min
R = fines destruction rate, $(Q_R + Q_P)/Q_P$
R' = $\overline{R}[1 + k_c(1 - i)]$
R_s = value of R at stability boundary
t = time, min
$U_b(L)$ = step function at b
V = slurry or crystallizer volume, l
V_L = clear liquor volume in crystallizer, l
$W(L)$ cumulative weight fraction to size L
X_F = $L_F/\overline{G}\tau$
X_p = $L_P/\overline{G}\tau$
y = log n

z = classifier flow rate, Q_z/Q_P

Greek Letters

α = $(z-a)/(L_p^+ - L_p^-)(2\overline{G}\tau)$
γ = $(Q_P + Q_{CLA})/Q_F$
ξ = $L/\overline{G}\tau$
ϵ = random error
ϵ_c = void or liquor fraction
ϵ_G = $1 - G/\overline{G}$
λ = $(R-1)X_F$
ρ = crystal density, g/cc
θ = time, t/τ
τ = residence time, V/Q_P, min
ω = frequency, 1/min

Superscript

$(^-)$ = steady state value

LITERATURE CITED

Bay, T., H. J. Kortright, and E. C. Muly, "Continuous Particle Size Analysis and Grinding Circuit Control," paper presented at ISA Meeting, Milwaukee, Wisc. (Oct., 1975).

Han, C. D., "A Control Study on Isothermal Mixed Crystallizers," Preprint 21A, Symposium on Selected Papers, Part I, 61st Annual Meeting, AIChE, Los Angeles, Calif. (1967).

Lei, S. J., R. Shinnar, and S. Katz, "The Stability and Dynamics of a Continuous Crystallizer with Fines Trap." *AIChE J.* **17**, 1459 (1971).

Nuttall, H. E., "Computer Simulation of Steady State and Dynamic Crystallizers," Ph.D. dissertation, Univ. Ariz., Tucson (1971).

Nyvlt, J., and J. W. Mullin, "The Periodic Behavior of Continuous Crystallizers," *Chem. Eng. Sci.*, **25**, 131 (1970).

Randolph, A. D., G. L. Beer, and J. P. Keener, "Stability of the Class II Classified Product Crystallizer with Fines Removal," *AIChE J.*, 19, 1140 (1973).

Randolph, A. D., and M. A. Larson, *Theory of Particulate Processes*, Chapt. 6, Academic Press, New York (1971).

Shields, J. P., "Transient Behavior in Crystallization-Design Models Related to Plant Experiences," unpublished (1976).

Timm, D. C., and G. Gupta, "Predictive-Corrective Control for Continuous Crystallization," Paper 18f, 63rd Annual Meeting, AIChE, Chicago, Ill. (1970).

APPENDIX

Consider the population balance as shown in Equation (4) along with the boundary condition of Equation (A1) with $j = 0$:

$$\frac{\partial n}{\partial t} + G\frac{\partial n}{\partial L} + \frac{nh(L)}{\tau} = 0 \tag{4}$$

$$n^0 = k_N G^{i-1} \tag{A1}$$

Magma independent nucleation ($j = 0$) is considered here in order to conform with the specific analysis of Figure 2 of Part I.

Define the following dimensionless variables and introduce these definitions into Equations (4) and (A1):

$$\xi = \frac{L}{\overline{G}\tau} \tag{A2}$$

$$\theta = t/\tau \tag{A3}$$

$$\epsilon_G = 1 - \frac{G}{\overline{G}} \tag{A4}$$

$$\frac{\partial n}{\partial \theta} + (1-\epsilon_G)\frac{\partial n}{\partial \xi} + h(\xi)n = 0 \tag{A5}$$

$$n^0 = \overline{n}^0(1-\epsilon_G)^{i-1} \tag{A6}$$

Define a population density deviation variable N:

$$N = \frac{n}{\overline{n}} - 1 \tag{A7}$$

Substituting Equation (A7) along with the steady state solution to Equation (A5) into Equation (A5) and reducing, we get

$$\frac{\partial N}{\partial \theta} + (1-\epsilon_G)\frac{\partial N}{\partial \xi} + (N+1)\,[h(\xi) + \epsilon_G\overline{h}(\xi)] = 0 \tag{A8}$$

with

$$N^0 = (1-\epsilon_G)^{i-1} - 1 \tag{A9}$$

Let $h(\xi) - \overline{h}(\xi)$ be defined as the withdrawal deviation function $H(\xi)$, and consider the case of small deviations in ϵ_G. Leaving terms of order ϵ_G, Equations (A8) and (A9) become

$$\frac{\partial N}{\partial \theta} + \frac{\partial N}{\partial \xi} + [H(\xi) + \epsilon_G\overline{h}(\xi)] = 0 \tag{A10}$$

$$N^0 = (1-i)\epsilon_G \tag{A11}$$

Consider a proportional control scheme where the nuclei density n^0 is the controlled variable and fines destruction rate R the manipulated variable This scheme is represented by Equation (A12):

$$\left[\frac{R}{\overline{R}} - 1\right] = K_c\left[\frac{n^0}{n^0} - 1\right] \tag{A12}$$

For small ϵ_G, Equation (A12) can be further reduced:

$$R - \overline{R} = K_c R N^0 \tag{A13}$$

$$R - \overline{R} = K_c\overline{R}(1-i)\epsilon_G \tag{A14}$$

The withdrawal function $h(\xi)$ is a step function in particle size L which can be expressed as

$$h(\xi) = R + (-R+1)U_{\xi F}(\xi) + (z-1)U_{\xi P}(\xi) \tag{A15}$$

To simplify the mathematics, define a shorthand notation for Equation (A15):

$$h(\xi) = \begin{bmatrix} R \\ 1 \\ z \end{bmatrix} \tag{A16}$$

The form of Equation (A16) will be used throughout the discussion to imply the form of Equation (A15).

Consider $H(\xi)$ and reduce it to a more usable form:

$$H(\xi) = h(\xi) - \overline{h}(\xi) \tag{A17}$$

$$H(\xi) = \begin{bmatrix} R \\ 1 \\ z \end{bmatrix} - \begin{bmatrix} \overline{R} \\ 1 \\ z \end{bmatrix} \tag{A18}$$

$$H(\xi) = \begin{bmatrix} R-\overline{R} \\ 0 \\ 0 \end{bmatrix} \tag{A19}$$

$$H(\xi) = \begin{bmatrix} K_c\overline{R}(1-i) \\ 0 \\ 0 \end{bmatrix}\epsilon_G \tag{A20}$$

Introduce Equation (A20) into Equation (A10) and simplify:

$$\frac{\partial N}{\partial \theta} + \frac{\partial N}{\partial \xi} + H(\xi)\epsilon_G = 0 \tag{A21}$$

with

$$N^0 = (1-i)\epsilon_G \tag{A11}$$

and

$$H(\xi) = \begin{bmatrix} \overline{R}[1 + K_c(1-i)] \\ 1 \\ z \end{bmatrix} \tag{A22}$$

First, consider the case of no control (for example, $K_c = 0$). For this case, $H(\xi)$ reduces to $\overline{h}(\xi)$. The stability picture for this case has previously been solved via spectral analysis by

Randolph et al. (1973) and is presented in Figure 2 of Part I. Now define $\overline{R}[1 + K_c(1 - i)]$ to be R', where R' is composed of system parameters. Therefore, Randolph et al. (1973) have already solved this case too. In fact, if R' is less than equal to R_s where R_s lies on the stability boundary line, then stability is guaranteed:

$$R' \leq R_s \qquad \text{(A23)}$$

or

$$R[1 + K_c(1 - i)] \leq R_s \qquad \text{(A24)}$$

Rearranging Equation (A24) we get the minimum K_c required for stability:

$$K_c \geq (1 - R_s/\overline{R})/(i - 1) \qquad (23)$$

Manuscript received December 6, 1976; revision received April 22, and accepted April 27, 1977.

Predicting the Combustion Rate of Pulverized Fuel from Its Initial Size Distribution

M. E. LEESLEY

Department of Chemical Engineering
University of Texas
Austin, Texas 78712

It is assumed that for pulverized fuel, the weight fraction W with a size larger than x can be expressed as $W = \exp(-bx^n)$. This paper describes the theoretical development and experimental evaluation using pulverized anthracite burning at 30 lb/hr of a method of predicting the combustion rate of a pulverized fuel from the constants b and n in the above equation.

SCOPE

This work was carried out to determine the effect of the initial particle size distribution of a pulverized fuel on its subsequent combustion rate.

With such a relationship available, it was felt that the designers of pulverized fuel firing equipment would be able to calculate the flame parameters that would result from a proposed comminution system. Before the work was undertaken, a substantial amount of data were available relating flame parameters to coal composition, coal-air ratios, flame turbulence and swirl, and combustion temperature and pressure, but nothing was known of the effect of size. Most workers had been deterred by the difficulties of obtaining sized fractions of coal in amounts large enough to sustain a large industrial flame for sufficient time to carry out the necessary measurements.

This work was made possible by the use of high throughput continuous sieving machines to provide the sized fractions and the one-dimensional experimental combustion technique developed by Beer and Thring (1961) which allows the stabilization of a flame with fuel feeds as low as 30 lb/hr.

CONCLUSIONS AND SIGNIFICANCE

The pulverized anthracite and twelve specially sized fractions made from it were burned individually in the experimental furnace. In all, 160 data points were collected. An attempt to correlate the results with conventional relationships for pulverized fuel combustion failed. The data appeared to be related by two separate expressions depending on whether polydisperse or monodisperse fractions of the fuel was burned.

A theoretical approach from basic concepts showed that both of the expressions were special cases of a general expression which was theoretically derived in the course of this work. The general expression could be written solely in terms of the initial particle size distribution of the raw, unsized fuel.

Both sets of experimental data showed good correlation when fitted to the new expression.

A designer of pulverized fuel burning systems is presented with a new tool. Experimental work must still be carried out to find the relationship between combustion